

Supplemental data for

Acylphloroglucinols biosynthesis in strawberry fruit

Chuankui Song¹, Ludwig Ring¹, Thomas Hoffmann¹, Fong-Chin Huang¹, Janet Slovin²,
Wilfried Schwab^{1*}

¹ Biotechnology of Natural Products, TU München, Liesel-Beckmann-Str.1, 85354
Freising, Germany

² USDA/ARS Genetic Improvement of Fruits and Vegetables Laboratory, BARC-W 10300
Baltimore Ave, Beltsville 20705, Maryland, USA

TABLE OF CONTENTS

Supplemental Tables

Supplemental Table S1. List of primers used in this study	3
Supplemental Table S2. Metabolites (<i>m/z</i> negative ionization mode and retention time) that were found to be differentially accumulated in strawberry fruit after down-regulation and overexpression of different genes.	4
Supplemental Table S3. Metabolites (<i>m/z</i> negative ionization and retention time) that were found to be differentially accumulated in strawberry fruit after down-regulation of <i>CHS</i> (<i>CHSi</i>)	4
Supplemental Table S4. ¹ H- and ¹³ C-NMR data derived from HSQC and HMBC data of isolated metabolite M1 and data from literature	5
Supplemental Table S5. ¹ H-NMR data derived from HSQC and HMBC data of isolated metabolite M3, and ¹ H-NMR data from literature	5

Supplemental Figures

Supplemental Figure S1. Relative mRNA expression level of candidate genes in different tissues	7
Supplemental Figure S2. Constructs used for this study	8
Supplemental Figure S3. Extracted ion chromatogram (<i>m/z</i> 357 and 371, superimposed), MS and MS2 spectra of metabolites M1, M2 and M3	9
Supplemental Figure S4. Relative expression levels of putative chalcone synthase genes in strawberry (<i>F. vesca</i> Hawaii-4) fruit tissue	10
Supplemental Figure S5. Comparison of the deduced amino acid sequences of CHS enzymes from <i>F. vesca</i>	11
Supplemental Figure S6. Phylogenetic tree of CHS/VPS enzymes	12
Supplemental Figure S7. LC-MS analysis of products formed by the empty vector control and FvCHS2-3 from the starter molecule 4-coumaroyl-CoA	13
Supplemental Figure S8. LC-MS analysis of products formed by the empty vector control and FvCHS2-1 from the starter molecule isovaleryl-CoA	14
Supplemental Figure S9. LC-MS analysis of products formed by the empty vector control and FvCHS2-1 from the starter molecule isobutyryl-CoA	15
Supplemental Figure S10. Products formed by FvCHS2-1 using 300 μ M malonyl-CoA and different concentrations of isovaleryl-CoA	16
Supplemental Figure S11. LC-MS analysis of the product formed by the empty vector control and FvCHS2-1 from the starter molecule feruloyl-CoA	17
Supplemental Figure S12. LC-MS analysis of products formed by the empty vector control and FvCHS2-3 from the starter molecule cinnamoyl-CoA	18
Supplemental Figure S13. The pH and temperature optima	19
Supplemental Figure S14. The effect of different amounts of protein (0.5-10 μ g) and incubation time (5 – 60 min) on the product formation of FvCHS2-3 using cinnamoyl-CoA as the starter substrate	20
Supplemental Figure S15. Michaelis-Menten plots of purified FvCHS2-3 with the substrate isobutyryl-CoA, 4-coumaroyl-CoA, isovaleryl-CoA, feruloyl-CoA and cinnamoyl-CoA	21
Supplemental Figure S16. Relative content of M1, M2 and M3 measured by LC-MS (n=3-5) and relative <i>CHS</i> expression (gene 26825 and gene 26826) determined by quantitative PCR	22
Supplemental Figure S17. Mass spectrum (MS) and MS2 of unlabeled M1 (A) and isotopically labeled M1 (B) after application of L-isoleucine- $^{13}\text{C}_6$, proposed pathway (C), as well as the effect of the incubation period on the accumulation of labeled product (D)	23
Supplemental Figure S18. Mass spectrum (MS) and MS2 of unlabeled M3 (A) and isotopically labeled M3 (B) after application of L-leucine- $^{13}\text{C}_6$, proposed pathway (C), as well as the effect of the incubation period on the accumulation of labeled product (D)	24
Supplemental Figure S19. Comparison of the deduced amino acid sequences of CHS enzymes from <i>F. vesca</i> , FvCHS2-1 and FvCHS2-2, as well as VPS and HICHSH1 from hop	25

Table S1. List of primers used in this study

Name	Forward primer	Purpose
Gene21343F	TCTTGCTACGAAATGCGATG	RT-qPCR
Gene21343R	TTTCACACAAGCAACTCTTCTGA	RT-qPCR
Gene10776F	GGTCCGAACACATCCTGAGT	RT-qPCR
Gene10776R	ATGATGGGGTATACCGATGG	RT-qPCR
Gene33865F	GATACAGAACATTCGGTGGGTTT	RT-qPCR
Gene33865R	CAAGCATATGACTACTGGCATGAT	RT-qPCR
Gene00897F	CACACCCACAGCTAGATAAGAGG	RT-qPCR
Gene00897R	AAACAGATGCACAGTTGCTTTCT	RT-qPCR
Gene23054F	AAAACGGGAACCAACATCAA	RT-qPCR
Gene23054R	CTACTGCTAGGGACAAAGATTGC	RT-qPCR
Gene35152F	TTGGTTGGGCTATGGATTGT	RT-qPCR
Gene35152R	AATCCCGCGATACCTCTACC	RT-qPCR
Gene03515F	ATTCAACTACGATATGCTCATGG	RT-qPCR
Gene03515R	G TTCAGCAATGGTGTATCAACAG	RT-qPCR
Gene27098F	CTGCATGGGTAAATGATAAGAGG	RT-qPCR
Gene27098R	CCAGTAACAGCATTAAGGAGAGC	RT-qPCR
Gene19724F	TTGCAATCTCTCTGGATCCTT	RT-qPCR
Gene19724R	CTCTCTGCGCTAACATGAAGAAC	RT-qPCR
Gene22502F	GTTGGACTTGGTCAAAGATTGAG	RT-qPCR
Gene22502R	AAGTGTGTAGATCAAACGCCTTC	RT-qPCR
Gene30399F	TTGGGTTAAGGGGATAGGTAGAG	RT-qPCR
Gene30399R	TGGTTAGGATGCTGATTCAAAC	RT-qPCR
Gene03472F	CCAGGTTGATTTCTCTTCGTAAA	RT-qPCR
Gene03472R	GGCGGTATCCATCTTAGAGAAGT	RT-qPCR
Gene21343Fo	CGC GGATCCTCTTGCTACGAAATGCGATG	RNAi
Gene21343Re	CCC AAGCTT TTTCAC ACA AGC AACTCT TCTGA	RNAi
Gene33865Fo	CGCGGATCCCGACCG GTCCACCTT ATG	RNAi
Gene33865Re	CCC AAGCTTGCCCTTCCGTCAATTCT	RNAi
Gene10776Fo	CGCGGATCCATGGCTGCAGTTGCTCAAGCG	Over expression(OE)
Gene10776Re	CGAGCTCCTAAGTTCGGATGTGATC	Over expression(OE)
Gene00897Fo	CGCGGATCCATGGAGAGTTTCATGCGT	Over expression(OE)
Gene00897Re	CGAGCTCTTAACAGTGTTTGGTGCAGAA	Over expression(OE)
Gene21343Fo-RNAi	AGA GGC ACC TAT GCC GAC TA	RT-qPCR(RNAi)
Gene21343Re-RNAi	CAT CGC ATT TCG TAG CAA GA	RT-qPCR(RNAi)
Gene33865Fo-RNAi	TCG ACG TGT GAT TCT AAG CG	RT-qPCR(RNAi)
Gene33865Re-RNAi	CAA GCA TAT GAC TAC TGG CAT GA	RT-qPCR(RNAi)
Gene10776Fo-OE	ATGATGGGGTATACCGATGG	RT-qPCR(OE)
Gene10776Re-OE	GGTCCGAACACATCCTGAGT	RT-qPCR(OE)
Gene00897Fo-OE	CACACCCACAGCTAGATAAGAGG	RT-qPCR(OE)
Gene00897Re-OE	AAACAGATGCACAGTTGCTTTCT	RT-qPCR(OE)
CHS2.1F(Gene26825)	CGCGGATCCATGGTGACCGTTGAGGAA	Whole Length CHS
CHS2.1R(Gene26825)	CCGGAATTCTCAAGCAGATACACTGTG	Whole Length CHS
CHS2.2F(Gene26826)	CGCGGATCCATGGTGACCGTCGAGGAA	Whole Length CHS
CHS2.2R(Gene26826)	CCGGAATTCTCAAGCAGCCACACTGTG	Whole Length CHS
CHS2.3-F	CGCGGATCCATGGTGACCGTCGAGGAA	Whole Length CHS
CHS2.3-R	CCGGAATTCTCAAGCAGCCACACTGTG	Whole Length CHS

Table S2. Metabolites (*m/z* negative ionization mode and retention time) that were found to be differentially accumulated in strawberry fruit after down-regulation of *CHS* (*CHSi*), gene21343 (*Expansin-A8-like*), and gene33865 (*Ephrin-A1-like*), and overexpression of gene10776 (*SRG1-like*) and gene00897 (*Defensin-like*) when compared with levels in the pBI-Intron-*GUS* control fruit (pBI)^a

<i>m/z</i>	retention times	CHSi vs pBI		gene21343 vs pBI		gene33865 vs pBI		gene10776 vs pBI		gene00897 vs pBI	
		Fold change	p-value	Fold change	p-value	Fold change	p-value	Fold change	p-value	Fold change	p-value
357 ^b	34.4	-17.1	0.00005	-6.2	0.00001	-5.0	0.00014	-5.4	0.00003	-5.9	0.00001
323	33.1	-28.1	0.00049	-118.8	0.00046	-9.1	0.00034	-9.5	0.00011	-109	0.00045
188	17.9	-54.6	0.00238	-81.7	0.00229	-24.7	0.00252	-27.6	0.00229	-85.8	0.00231
321	36.8	-184.2	0.00261	-62.2	0.00263	-6.2	0.00401	-5.3	0.00315	-109.2	0.00262
664	18.0	-65.5	0.00275	-55.3	0.00272	-5.5	0.00273	-20.9	0.00264	-255.8	0.00264
313	33.1	-31.1	0.00281	-77.9	0.00262	-16.9	0.00302	-21.5	0.00283	-88.3	0.00262
455	31.7	-33.8	0.00397	-43.3	0.00387	-7.3	0.00547	-8.6	0.00307	-59.9	0.00379
771	40.2	-86.8	0.00608	-38.1	0.00637	-20.2	0.00685	-360.4	0.0059	-72.4	0.00612
496	18.1	-15.3	0.00764	-17.1	0.00701	-5.1	0.00959	-7.7	0.00726	-32.3	0.00675

^a Fold change and p-values are shown as calculated by XCMS for the pairwise comparison.

^b This metabolite was identified as M2

Table S3. Metabolites (*m/z* negative ionization and retention time) that were found to be differentially accumulated in strawberry fruit after down-regulation of *CHS* (*CHSi*) when compared with levels in the pBI-Intron-*GUS* control fruit (pBI)

<i>m/z</i>	retention time	CHSi vs PBI	p-value
715	34.28	-17.1	5.00E-05
435	37.17	-5.3	8.00E-05
309	32.95	-5.8	0.00036
565	34.30	5.4	0.00042
709	32.49	23.9	5.00E-04
355	32.93	-6.7	0.00062
356	32.96	-6.7	0.00109
661	34.25	-16.7	0.00173
347	33.00	-8.1	0.00193
345	32.96	-5.5	0.0028
371 ^a	38.27	-5.6	0.00305
389	32.43	7.5	0.00308
399	32.42	15	0.00404
709	32.47	26.9	0.00771
664	18.05	-23.3	0.00926
371 ^b	37.10	-6.4	0.01726

^{a, b} Metabolites were identified as M1 and M3, respectively

Table S4. ^1H - and ^{13}C -NMR data derived from HSQC and HMBC data of isolated metabolite M1 and data from literature

M1						
Atom	δH	Splitting	Bohr et al., 2005	δC	HMBC	Bohr et al., 2005
1				162.9		161.8
2				107.0		106.8
3				167.3		167.4
4	5.98	d	5.94 d 1H	99.3	C-6,C-5,C-3	98.3
5				165.6		165.6
6	6.20	d	6.17 d 1H	96.4	C-2,C-1,C-5	95.3
1'				211.8	C-2',C-3';C-5'	211.8
2'	3.93	m	3.90 m 1H	47.0	C-3',C-4;C-5'	47.0
3'	1.81, 1.40	m	1.80, 1.38 m 1H	28.3	C-4;C-5'	28.3
4'	0.90	t	0.87 t 3H	12.0	C-2',C-3;C-5'	12.0
5'	1.15	d	1.12 d 3H	16.8		16.8
1''	5.01	d	5.03 d 1H	101.7	C-2''	101.7
2''-5''	3.5-4.0	m	3.38 - 3.91 m	70-78		71.2 - 78.7
6''	3.70	dd	3.71	62.5		62.5

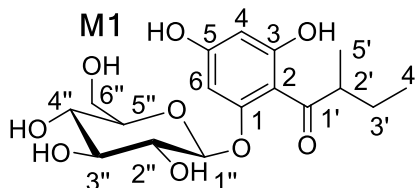
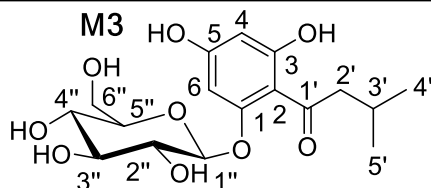


Table S5. ^1H -NMR data derived from HSQC and HMBC data of isolated metabolite M3, and ^1H -NMR data from literature (refer also to Aziz-ur-Rehman et al., 2005 and Gao et al., 2004)

M3				
H-Atom	Chemical shifts δH	Splitting,	Bohr et al., 2005	Tsukamoto et al., 2004
4	5.98	1H d	5.94 d 1H	5.93 d 1H
6	6.20	1H d	6.17 d 1H	6.15 d 1H
2'	3.14	2H 2dd	2.88 dd 1H, 3.17 dd 1H	2.87 dd 1H, 3.16 dd 1H
3'	1.82	1H sept	2.24 sept 1H	2.24 sept 1H
4' u.5'	0.91	6H dd	0.93 d 3H, 0.96 d 3H	0.92 d 3H, 0.96 d 3H
1''	5.05	1H d	5.01 d 1H	5.01 d 1H
2''-6''	3.5 - 4.0	m	3.39 - 3.91 m	3.39 - 3.91 m



Bohr, G., Gerhäuser, C., Knauft, J., Zapp, J., and Becker, H. (2005) Anti-inflammatory acylphloroglucinol derivatives from hops (*Humulus lupulus*). *J. Nat. Prod.* **68**: 1545–1548.

Tsukamoto, S., Tomise, K., Aburatani, M., Onuki, H., Hirorta, H., Ishiharajima, E., and Ohta, T. (2004) Isolation of cytochrome P450 inhibitors from strawberry fruit, *Fragaria ananassa*. *J. Nat. Prod.* **67**: 1839–1841.

Aziz-Ur-Rehman, M., Riaz N., Ahmad H., Nawaz S.A., and Choudhary M.I. (2005) Lipoxygenase inhibiting constituents from *Indigofera hetrantha*. *Chem. Pharm. Bull.* **53**: 263-266.

Gao, S., Feng, N., Yu, S., Yu De, Wang X. (2004) Vasodilator constituents from the roots of *Lysidice rhodostega*. *Planta Med.* **70**: 1128-1134.

Figures

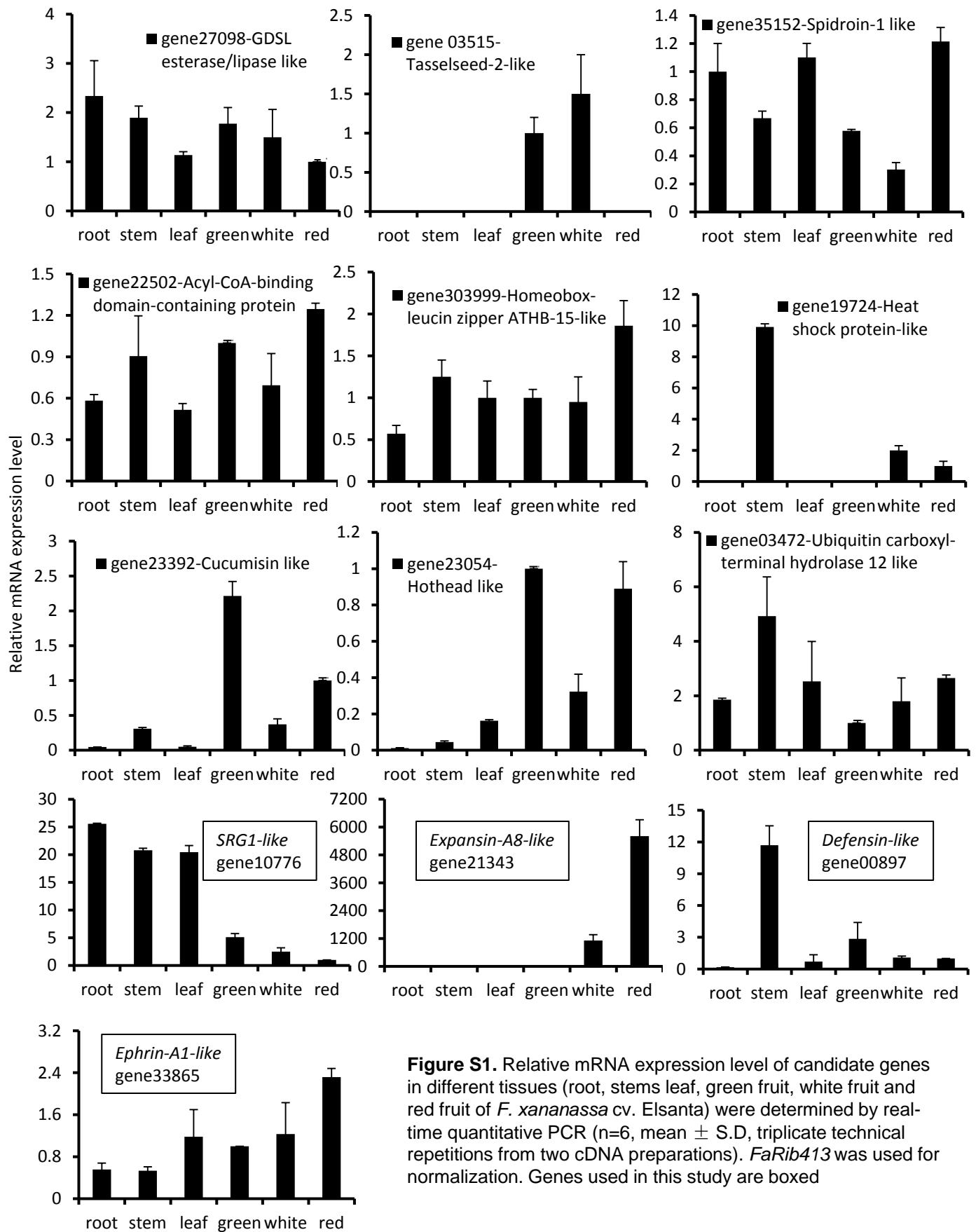
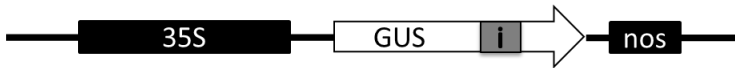
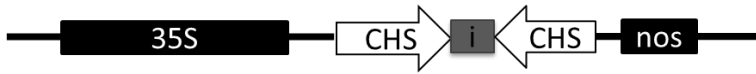


Figure S1. Relative mRNA expression level of candidate genes in different tissues (root, stems leaf, green fruit, white fruit and red fruit) of *F. xananassa* cv. Elsanta) were determined by real-time quantitative PCR (n=6, mean \pm S.D, triplicate technical repetitions from two cDNA preparations). *FaRib413* was used for normalization. Genes used in this study are boxed

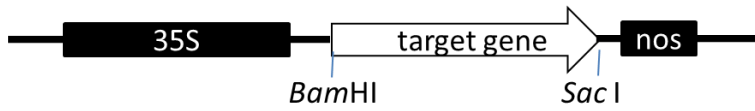
pBI-Intron: used for negative control



pBI-CHSi: used for positive control



pBI-target gene: used for over expression



P9U10-target gene: used for silencing

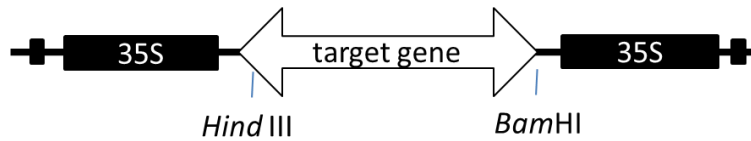


Figure S2. Constructs used for this study

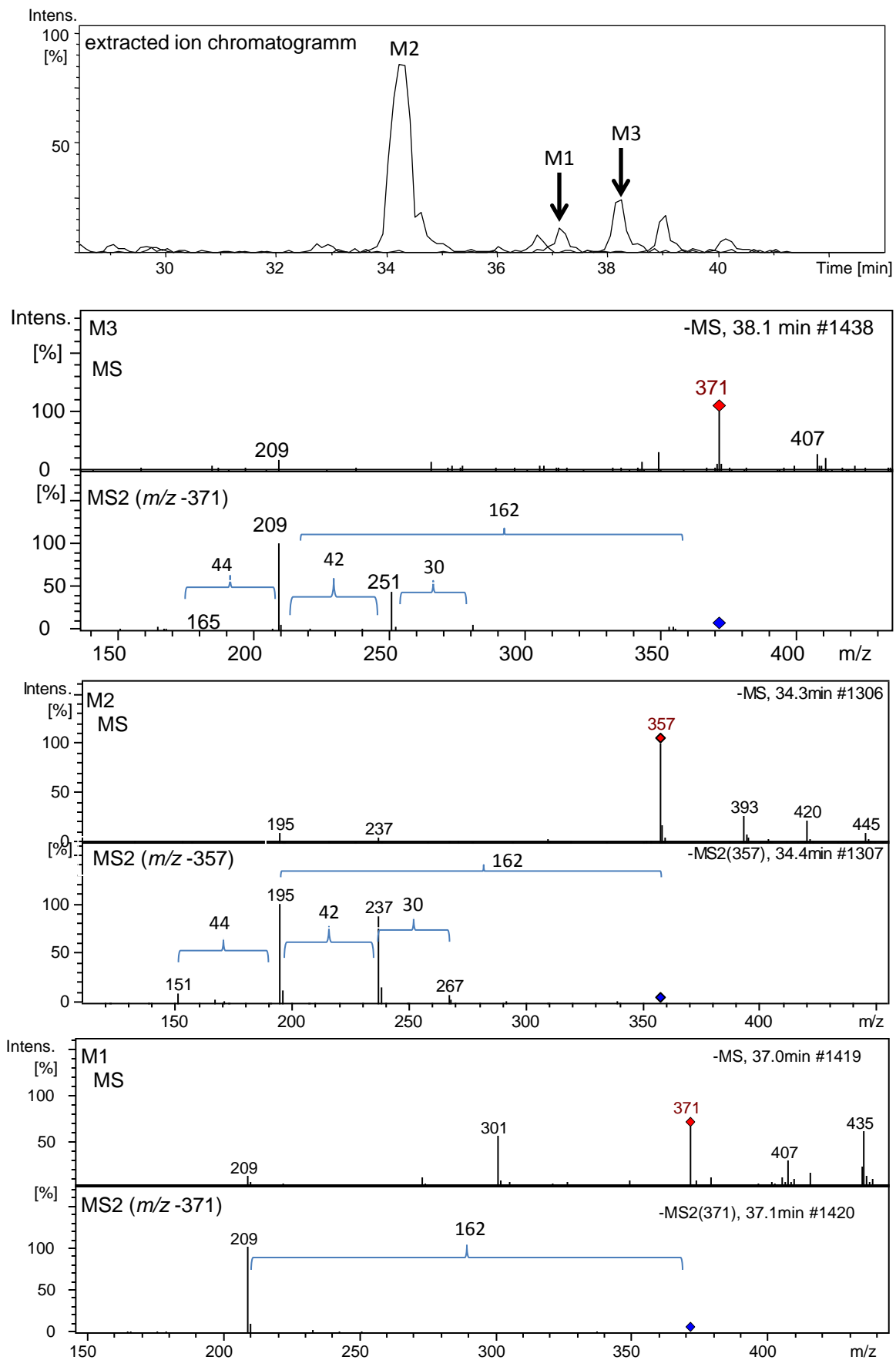


Figure S3. Extracted ion chromatogram (m/z 357 and 371, superimposed), MS and MS2 spectra of metabolites M1, M2 and M3.

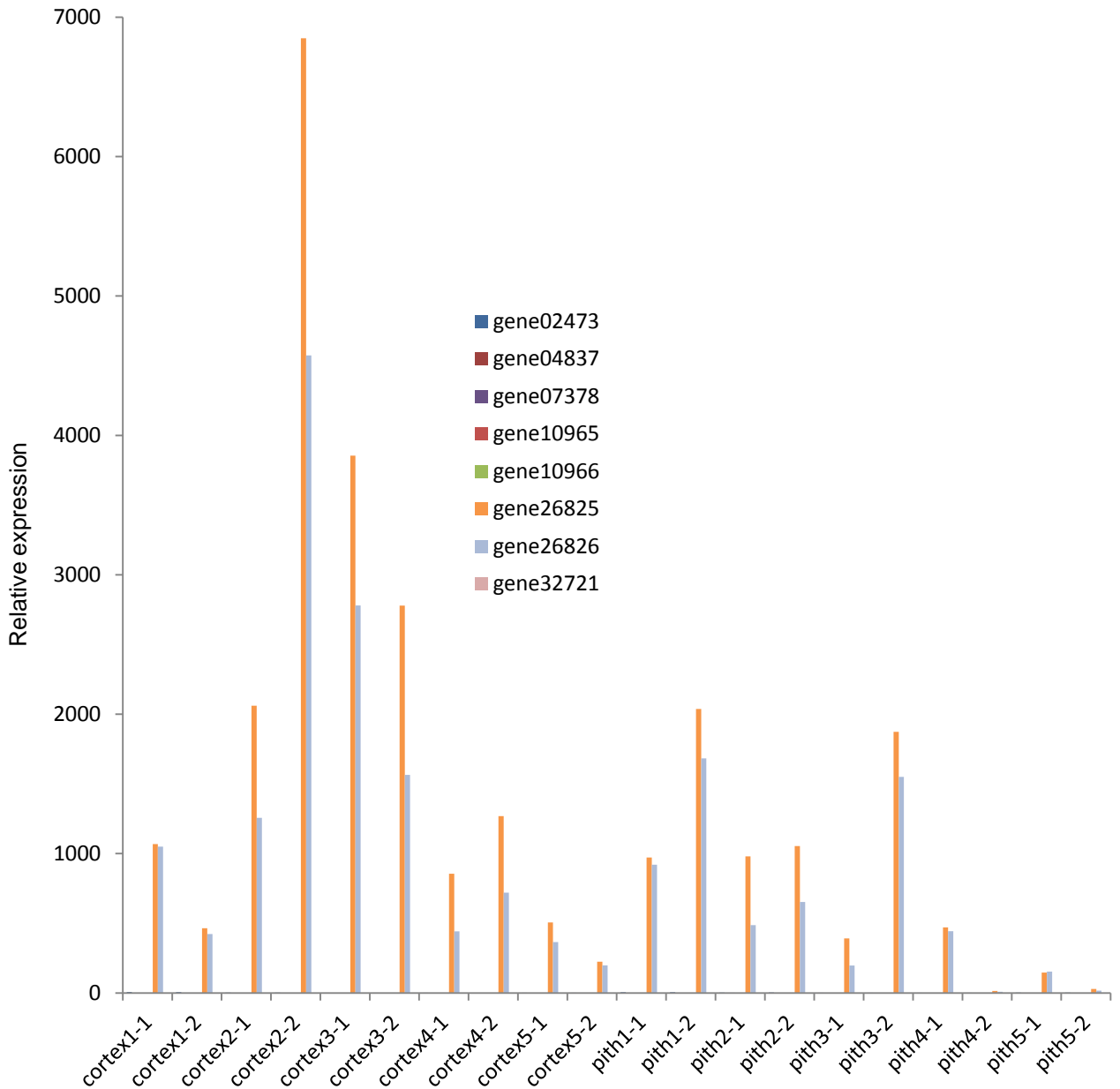


Figure S4. Relative expression levels of eight putative chalcone synthase genes in strawberry (*F. vesca* Hawaii-4) fruit tissue (cortex and pith) during early stages of fruit development (Kang et al., 2013). Only gene 26825 and 26826 is expressed. Transcripts of the other six genes were not detected in any of the materials tested. “Cortex1-1” represents “cortex-stage1-replicate1”. Stage 1: prefertilization stage, stage 2: 2 to 4 d postanthesis, stage 3: complete loss of anthers, and a heart stage embryo inside each seed, stage 4: embryos adopt torpedo or walking stick morphology, stage 5: embryos and achenes maturation. For details refer to http://bioinformatics.towson.edu/strawberry/newpage/Search_By_Gene_Desc.aspx

			10	20	30	40	50
FvCHS2-1	1	MVTVEEVRKA	QRAEGPATVL	AIGTATPPNC	IDQSTYPDYY	FRITNSEHKA	
FvCHS2-2	1	
FvCHS2-3	1	
			60	70	80	90	100
FvCHS2-1	51	ELKEKFQRM	DKSMIKKRYM	YLTEEILKEN	PSMCEYMAPS	LDARQDMVVV	
FvCHS2-2	51	
FvCHS2-3	51	
			110	120	130	140	150
FvCHS2-1	101	EIPKLGKDA	VKAIKEWGQP	KSRITHLVFC	TTSGVDMPGA	DYQLTKLLGL	
FvCHS2-2	101E..K.....	
FvCHS2-3	101	
			160	170	180	190	200
FvCHS2-1	151	RPSVKRLMM	YQQGCFAGGT	VLRLAKDLA	ENNRGARVL	VVVCSEITAV	TFRG
FvCHS2-2	151	
FvCHS2-3	151	
			210	220	230	240	250
FvCHS2-1	201	PSDTHLDSL	VGQALFGDGA	AIIIVGSDPL	P EVERPLFEL	V SAAQTILPD	S
FvCHS2-2	201	
FvCHS2-3	201	
			260	270	280	290	300
FvCHS2-1	251	DGAIDGHLR	E VGLTFHLLK	D VPGLISKNI	E KSLNEAFKPL	NITDWN	SLFW
FvCHS2-2	251	
FvCHS2-3	251	
			310	320	330	340	350
FvCHS2-1	301	IAHPGGPAIL	DQVEAKLALK	PEKLEATRHI	LSEYGNMSSA	CVLFILDEVR	
FvCHS2-2	301	
FvCHS2-3	301	
			360	370	380	390	
FvCHS2-1	351	RKSAANGHKT	TGEGLEWGV	L FGFPGGLT	VE TVVLH	SVSA*	
FvCHS2-2	351	.R.....K.....A.*	
FvCHS2-3	351	.R.....K.....A.*	

Figure S5. Comparison of the deduced amino acid sequences of CHS enzymes from *F. vesca*. FvCHS2-1 (gene26825) and FvCHS2-2 (gene26826) are chalcone synthases from *F. vesca*. FvCHS2-3 is a third protein whose corresponding gene was cloned from *F. vesca* fruit. The sequences were aligned using the ClustalW program. The highly conserved active site loop of CHS enzymes, G³⁷²FGPG and two Phe residues (Phe215 and Phe265), important in determining the substrate specificity of CHS are boxed.

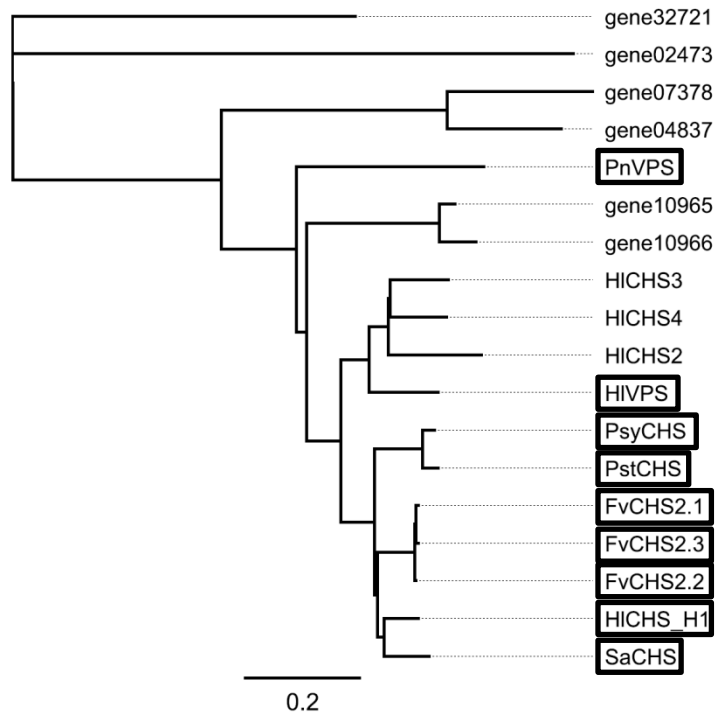


Figure S6. Phylogenetic tree of CHS/VPS enzymes and homologues from *F. vesca* and *Humulus lupulus* as well as functionally characterized CHS proteins with VPS promiscuous catalytic activity, generated by the Geneious (Pro 5.5.4) Tree Builder (Jukes Cantor genetic distance model and neighbor-joining method). The scale bar indicates the average number of amino acid substitutions per site. FvCHS2-1 *F. vesca* chalcone synthase 2-1 (XM_004306495.1; gene 26825), FvCHS2.2 *F. vesca* chalcone synthase 2.2 (XM_004306494.1; gene26826), FvCHS2-3 *F. vesca* chalcone synthase 2-3 (chimera of 2-1 and 2-2), PsyCHS *Pinus sylvestris* chalcone synthase (P30079), PstCHS *Pinus strobus* chalcone synthase (O65872), SaCHS *Sinapis alba* chalcone synthase (P13416), PnVPS *Psilotum nudum* valerophenone synthase (Q9SLX9), HICHS2-4 *Humulus lupulus* chalcone synthase 2-4 (AB061020, AB061022, CAD23044), HIVPS *Humulus lupulus* valerophenone synthase (O80400), HICHS_H1 *Humulus lupulus* chalcone synthase_H1 (CAC19808), gene02473, 04837, 07378, 10965, 10966, and 32721 are translated protein sequences of putative *F. vesca* chalcone synthases (Shulaev et al., 2011). Proteins with biochemically verified VPS activity are boxed.

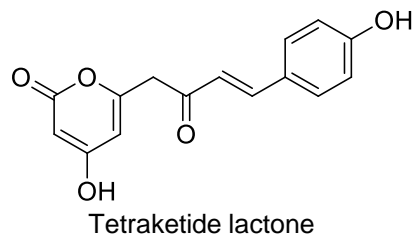
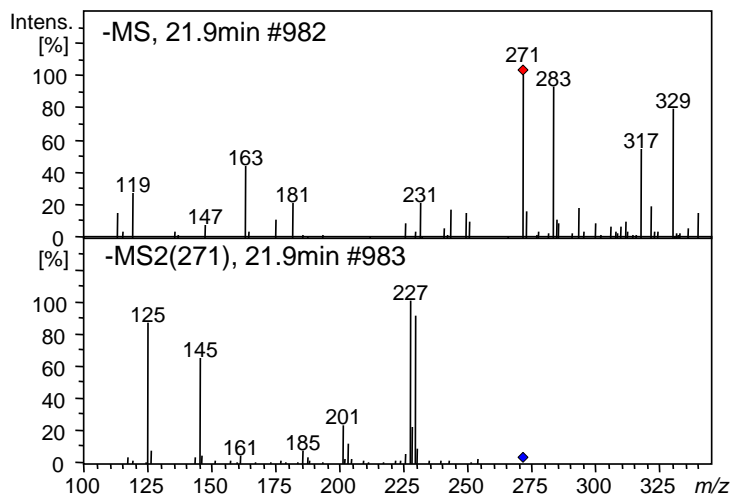
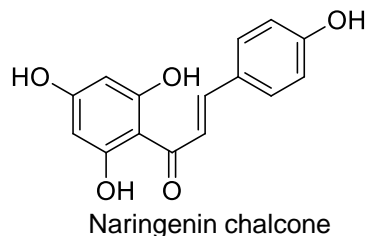
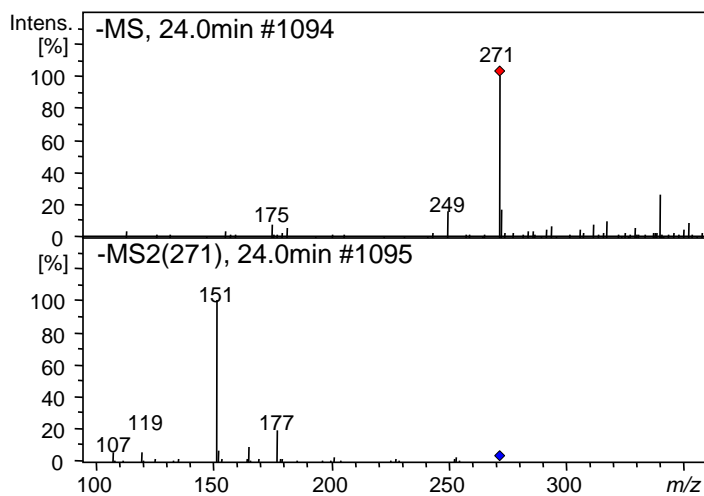
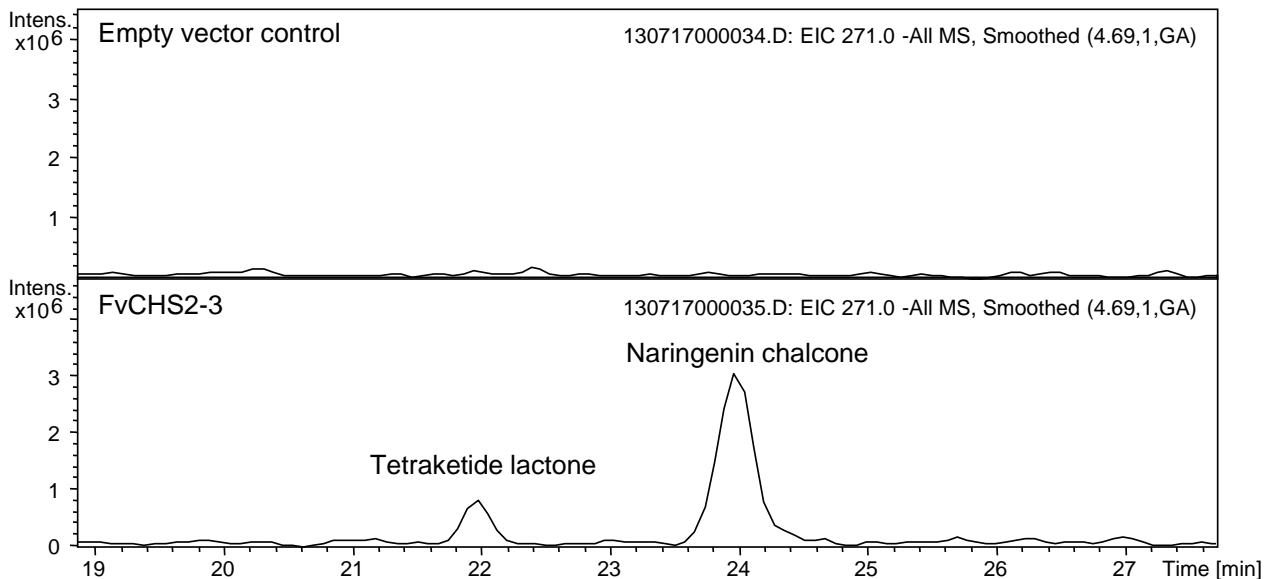


Figure S7. LC-MS analysis of products formed by the empty vector control and FvCHS2-3 from the starter molecule 4-coumaroyl-CoA. MS and MS2 spectra of naringenin chalcone and tetraketide lactone.

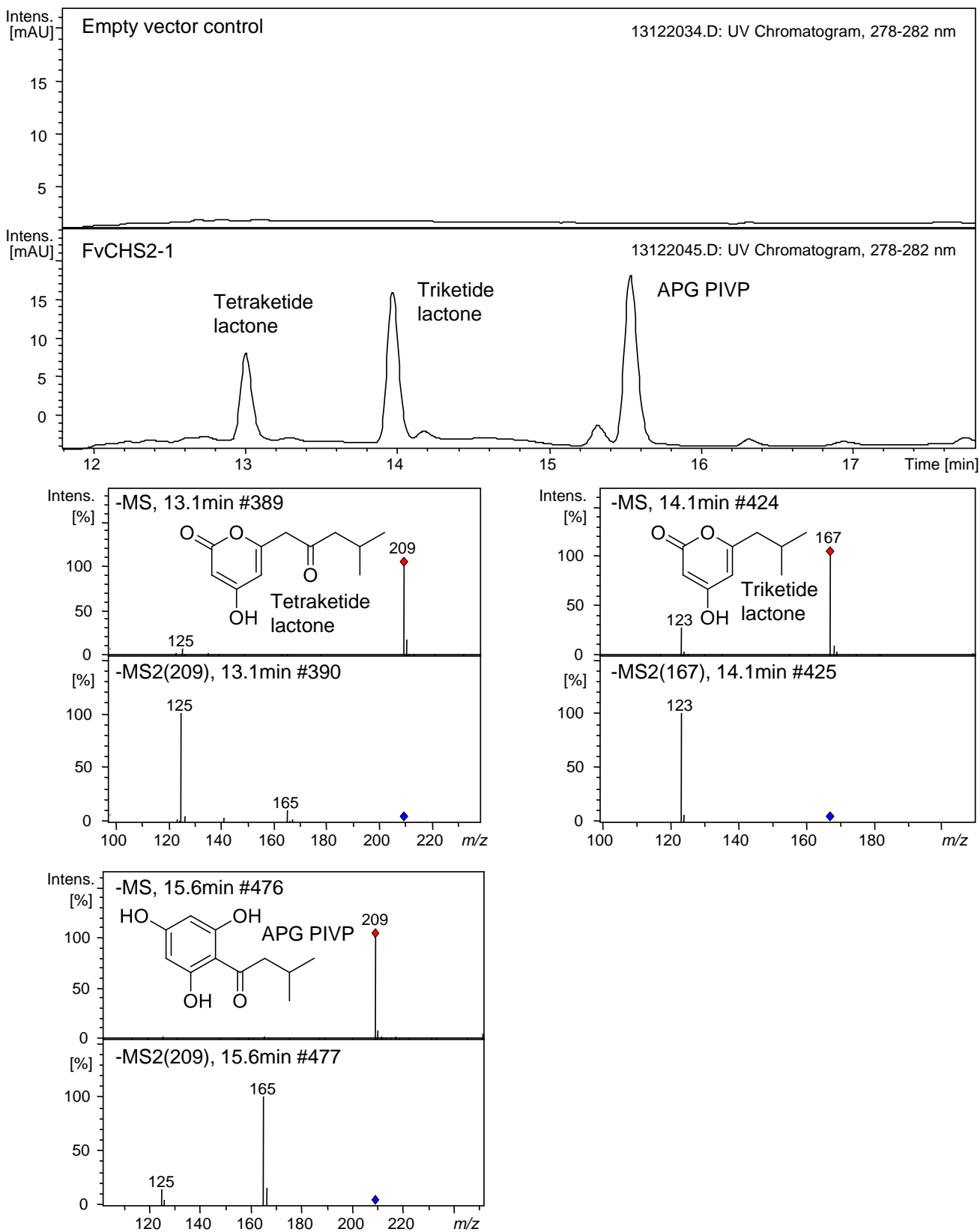


Figure S8. LC-MS analysis of products formed by the empty vector control and FvCHS2-1 from the starter molecule isovaleryl-CoA (UV trace). MS and MS2 spectra of tetraketide lactone, triketide lactone and APG (acylphloroglucinol). PIVP phlorisovalerophenone.

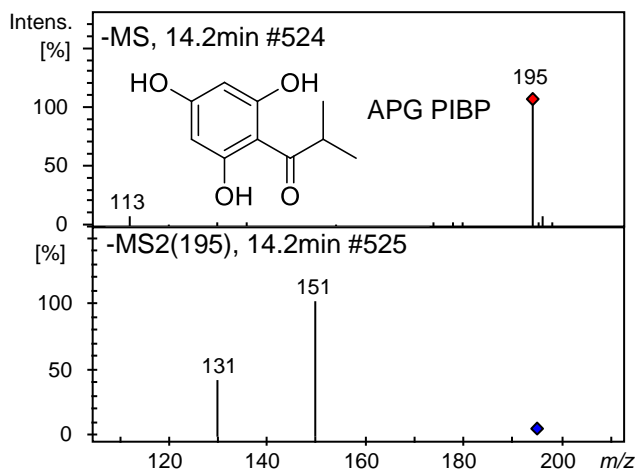
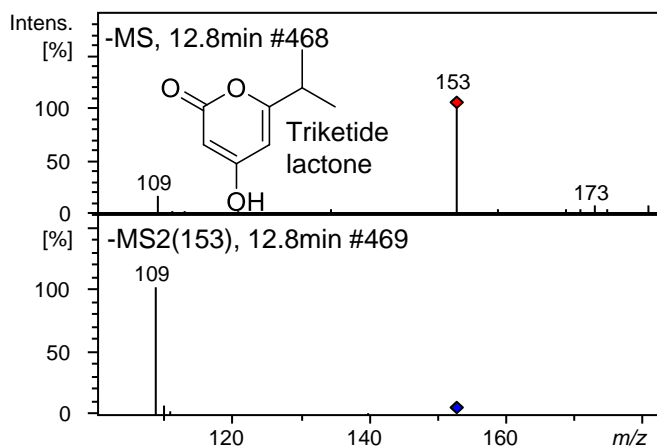
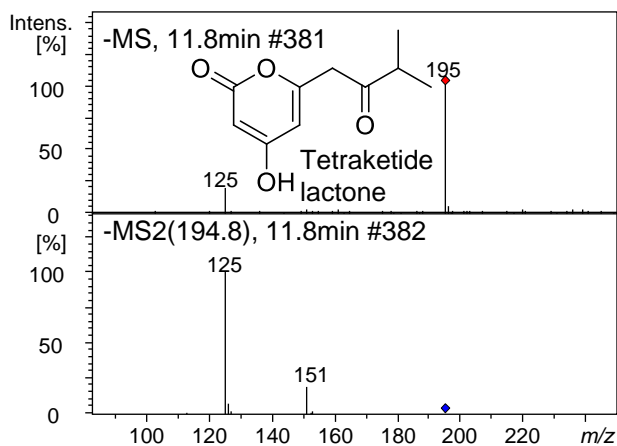
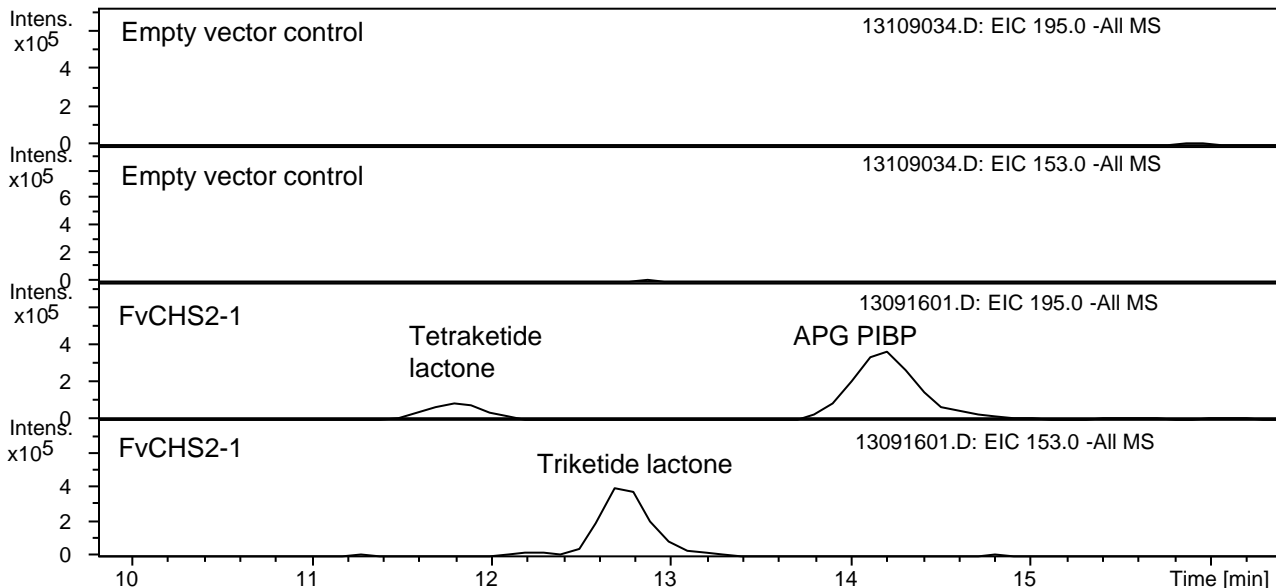


Figure S9. LC-MS analysis of products formed by the empty vector control and FvCHS2-1 from the starter molecule isobutyryl-CoA. MS and MS2 spectra of tetraketide lactone, triketide lactone and APG (acylphloroglucinol). PIBP phlorisobutyrophenone.

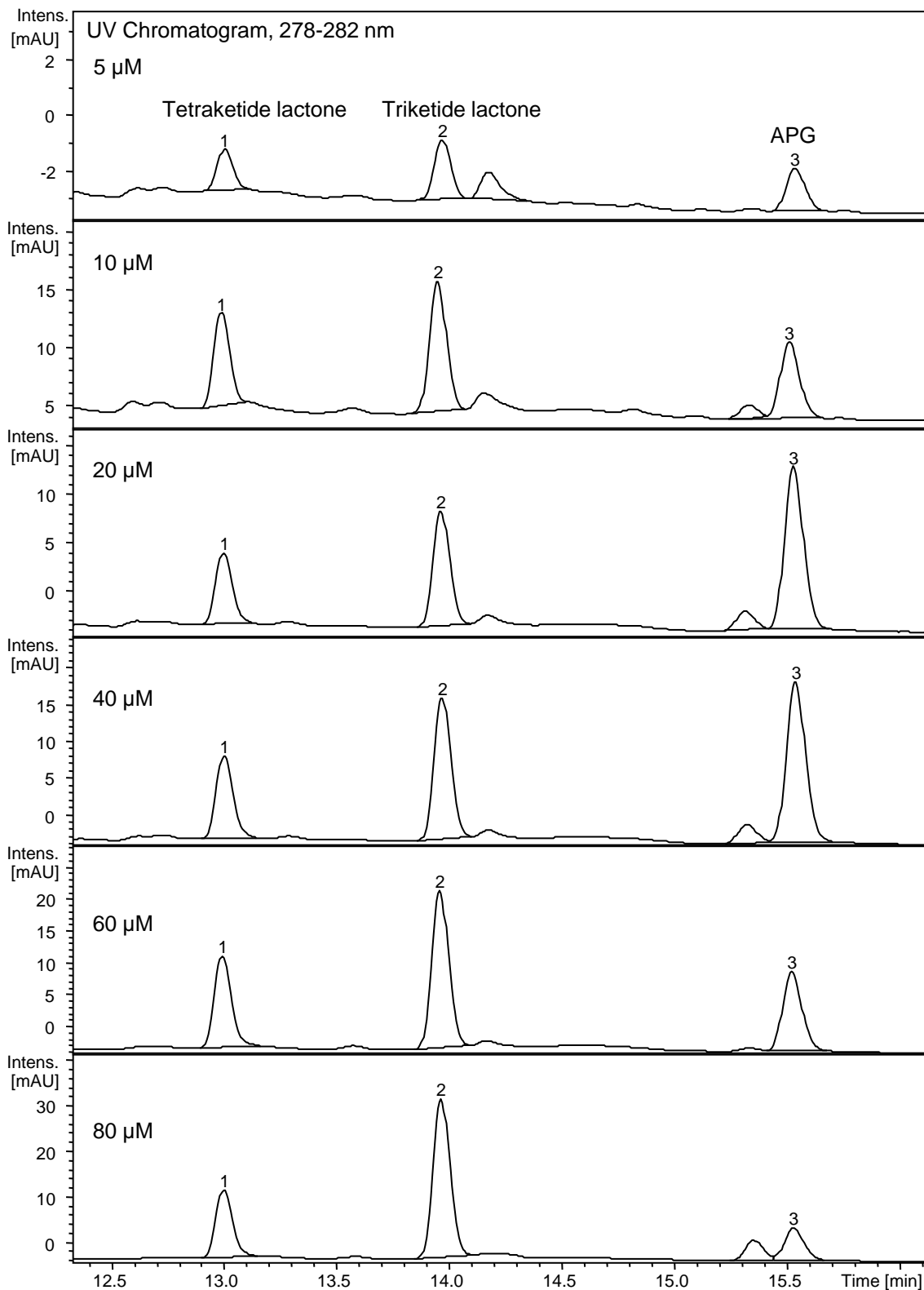


Figure S10. Products (tetraketide lactone 1, triketide lactone 2 and APG 3; signals at 14.3 and 15.4 min are unknowns) formed by FvCHS2-1 using 300 μM malonyl-CoA and different concentrations of isovaleryl-CoA (5, 10, 20, 40, 60, and 80 μM). The ratio of APG 3 is highest when the concentration of isovaleryl-CoA is 20 - 40 μM .

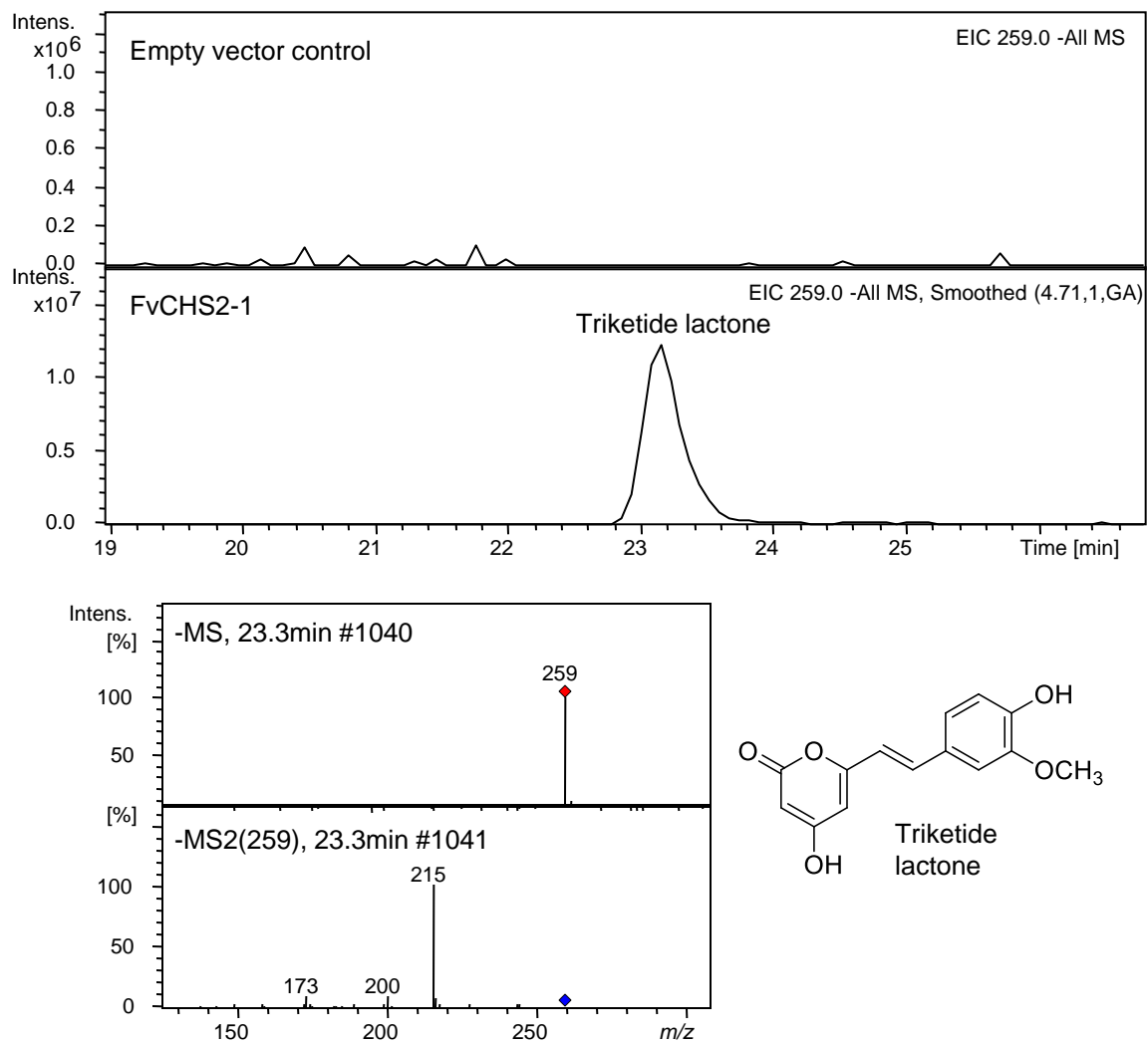


Figure S11. LC-MS analysis of the product formed by the empty vector control and FvCHS2-1 from the starter molecule feruloyl-CoA. MS and MS2 spectra of the triketide lactone.

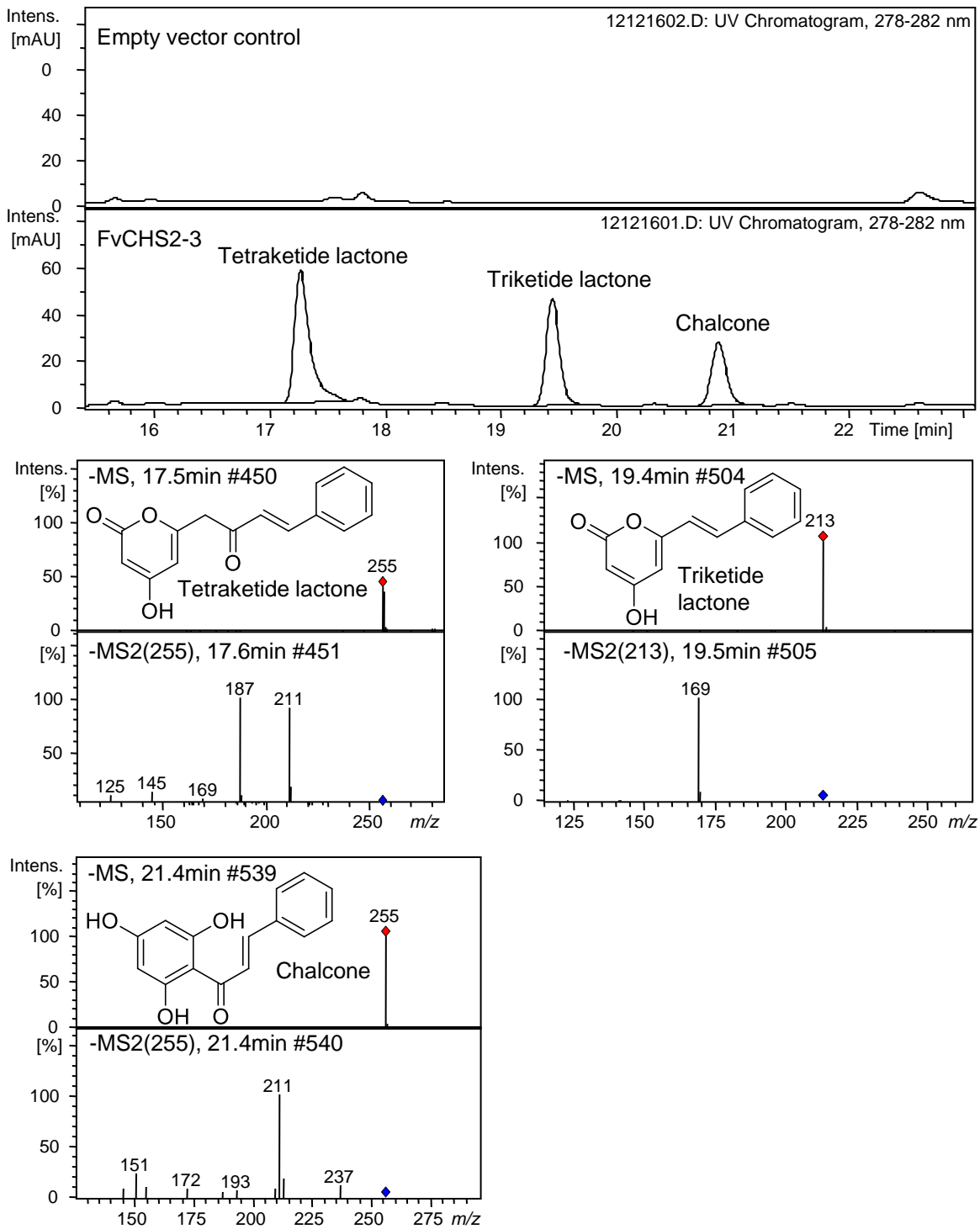


Figure S12. LC-MS analysis of products formed by the empty vector control and FvCHS2-3 from the starter molecule cinnamoyl-CoA. MS and MS2 spectra of tetraketide lactone, triketide lactone and chalcone.

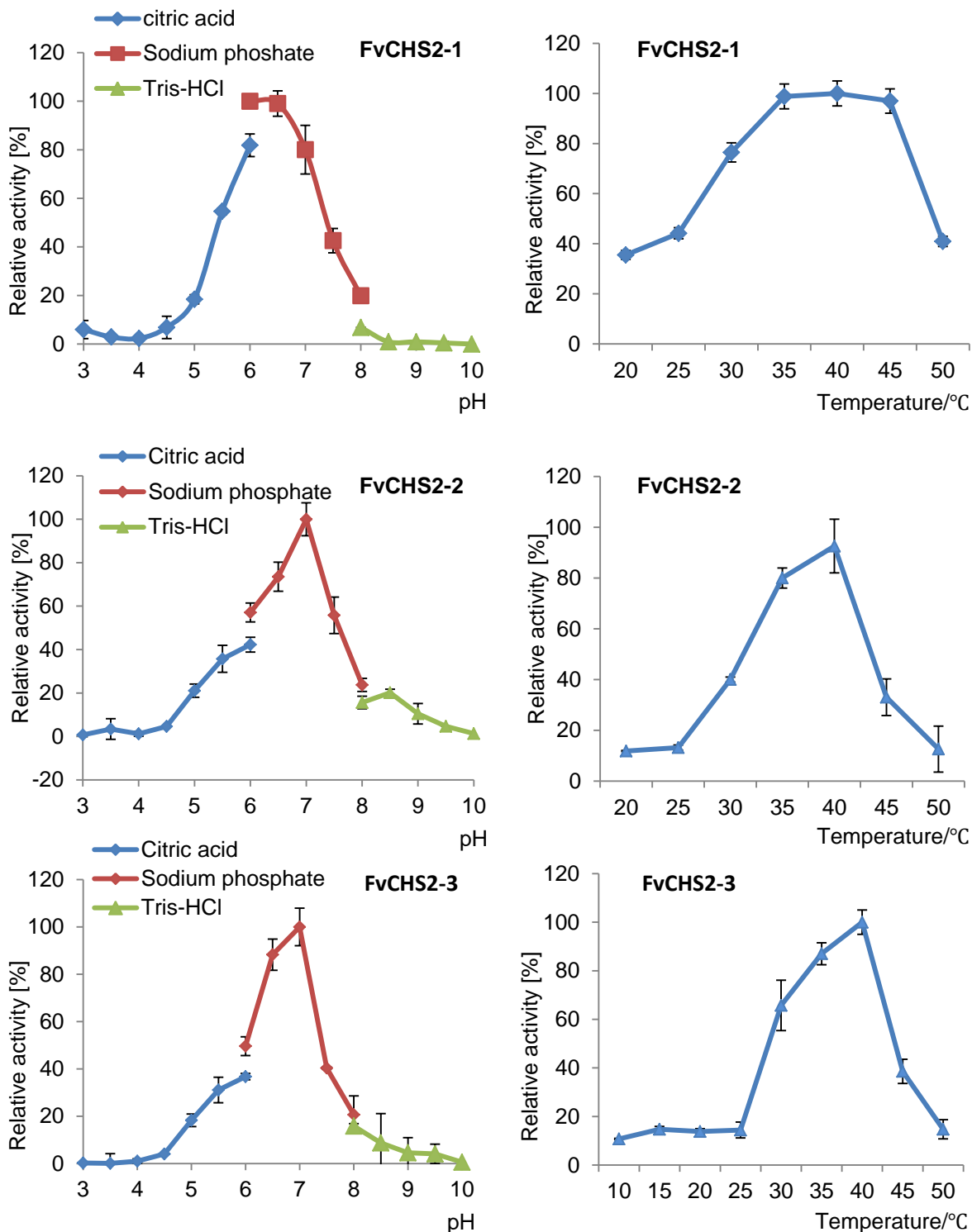


Figure S13. The pH and temperature optima. The purified enzymes (FvCHS2-1 – 2-3) were incubated with 100 μ M isovaleryl-CoA at 30 °C and different pH values (left column) and at pH 7.0 and different temperature values (right column). Citric acid buffer was used for pH 3 to 6, sodium phosphate buffer was used for pH 6 to 8, Tris-HCl buffer was used for pH 8 to pH 10. Temperature optima were determined in the range of 10 to 50 °C and was carried out at pH 7.0 for 10 min. Product formation was quantified by LC–MS analysis allowing the calculation of the Michaelis–Menten equation by hyperbolic regression and quantified as activity ($\text{pmol mg}^{-1} \text{s}^{-1}$).

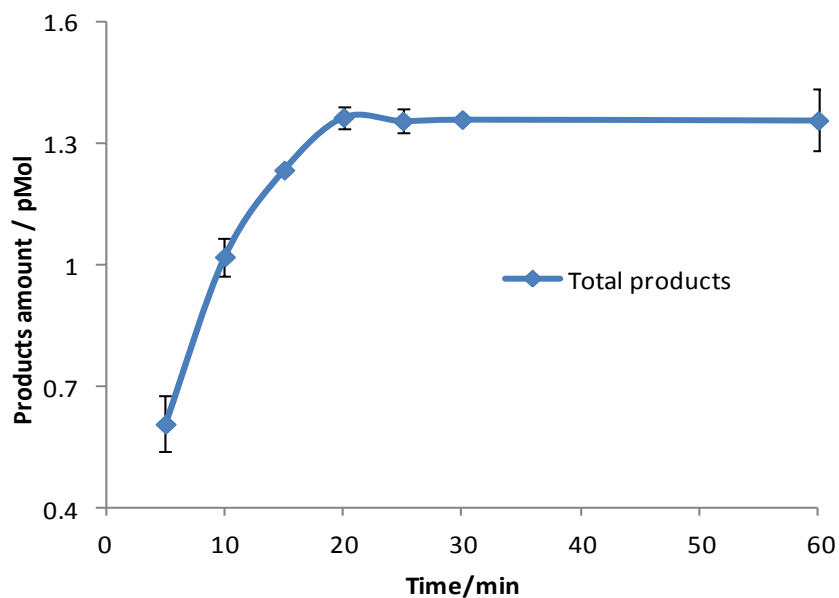
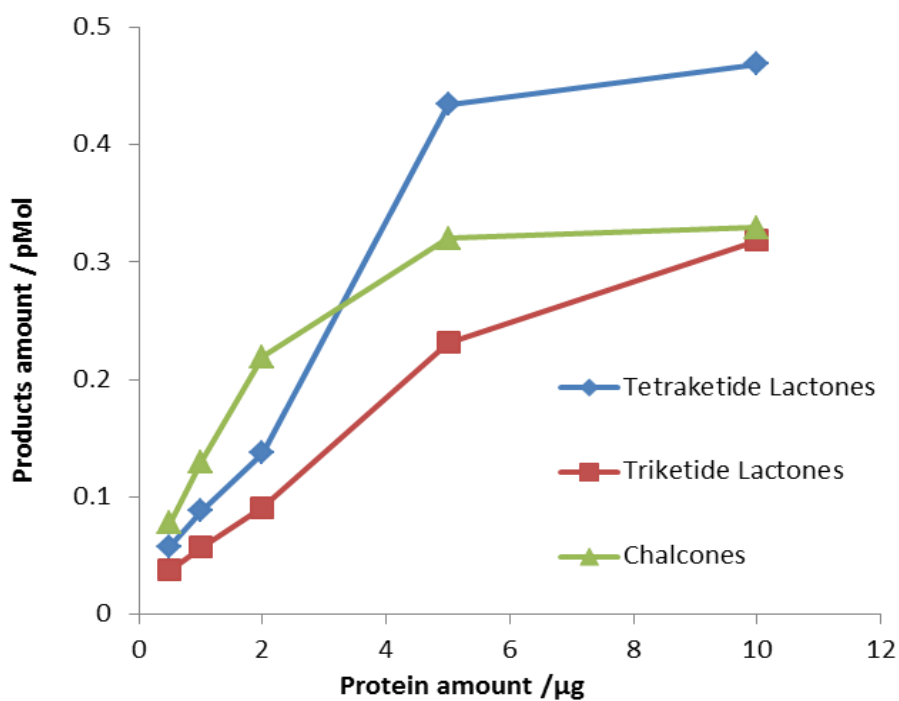


Figure S14. The effect of different amounts of protein (0.5-10 μg) and incubation time (5 – 60 min) on the product formation of FvCHS2-3 using cinnamoyl-CoA as the starter substrate. Naringenin (10 $\mu\text{g/ml}$) was used as an internal standard for quantification by LC-MS.

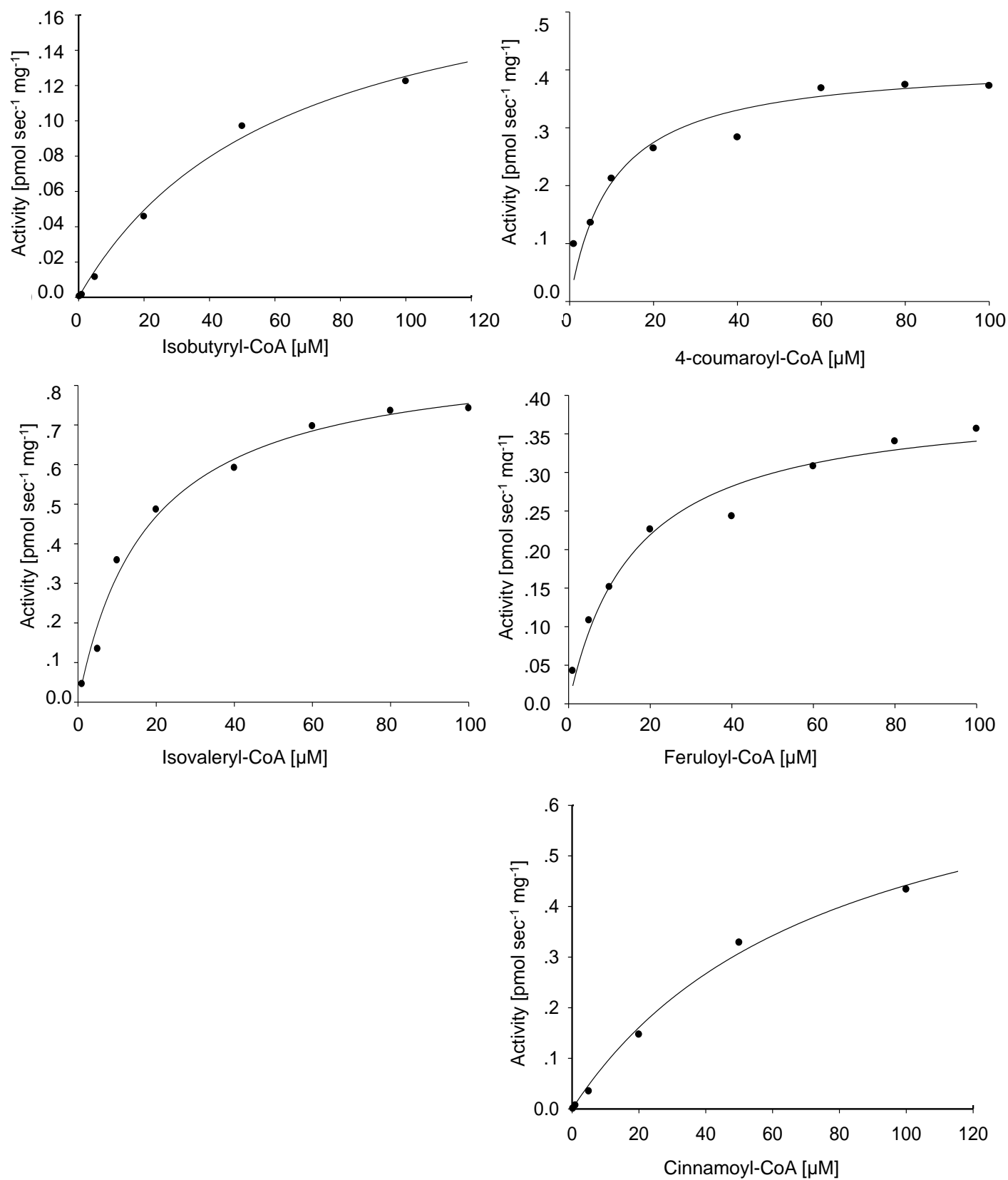


Figure S15. Michaelis-Menten plots of purified FvCHS2-3 with the substrate isobutyryl-CoA, 4-coumaroyl-CoA, isovaleryl-CoA, feruloyl-CoA and cinnamoyl-CoA. Activity ($\mu\text{mol s}^{-1} \text{mg}^{-1}$) was used to draw the plots and calculate the kinetic parameters.

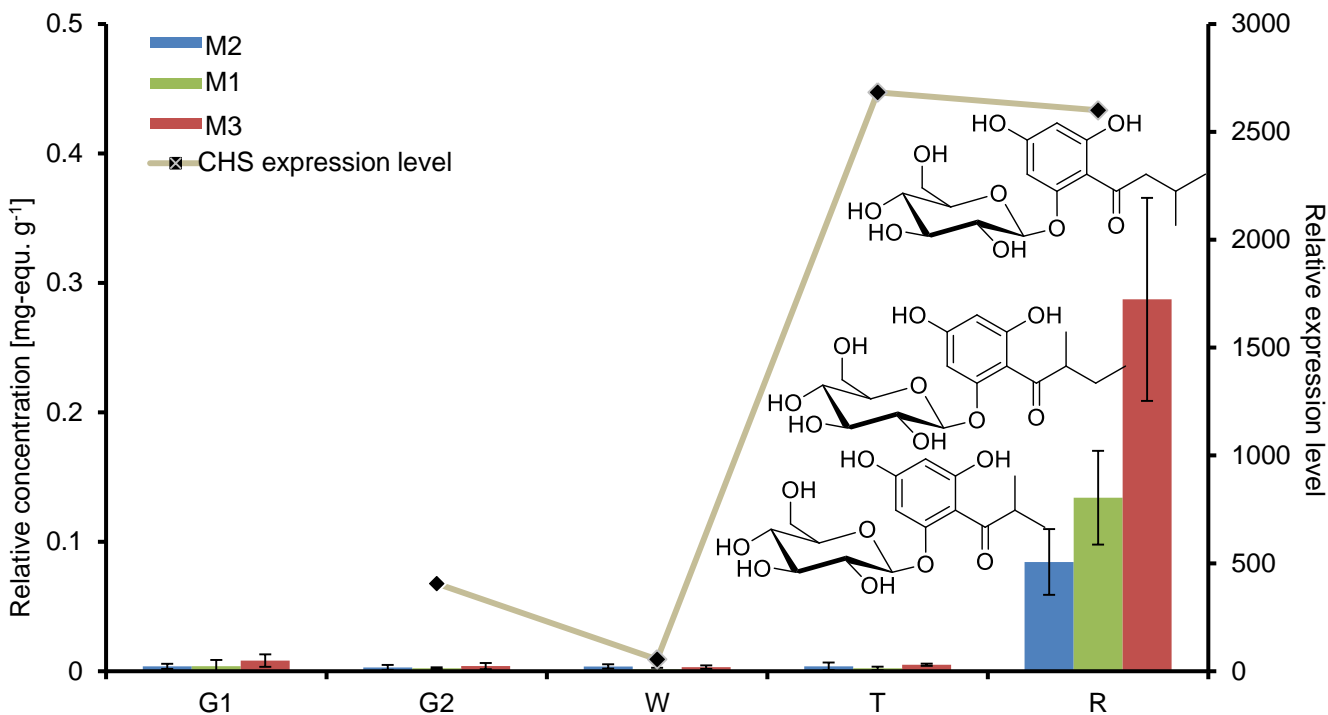


Figure S16. Relative content of M1, M2 and M3 measured by LC-MS (n=3-5) and relative *CHS* expression (gene 26825 and gene 26826) determined by quantitative PCR during strawberry fruit ripening (small green G1, large green G2, white W, turning T, red R of *F. x ananassa* cv. Mara des Bois).

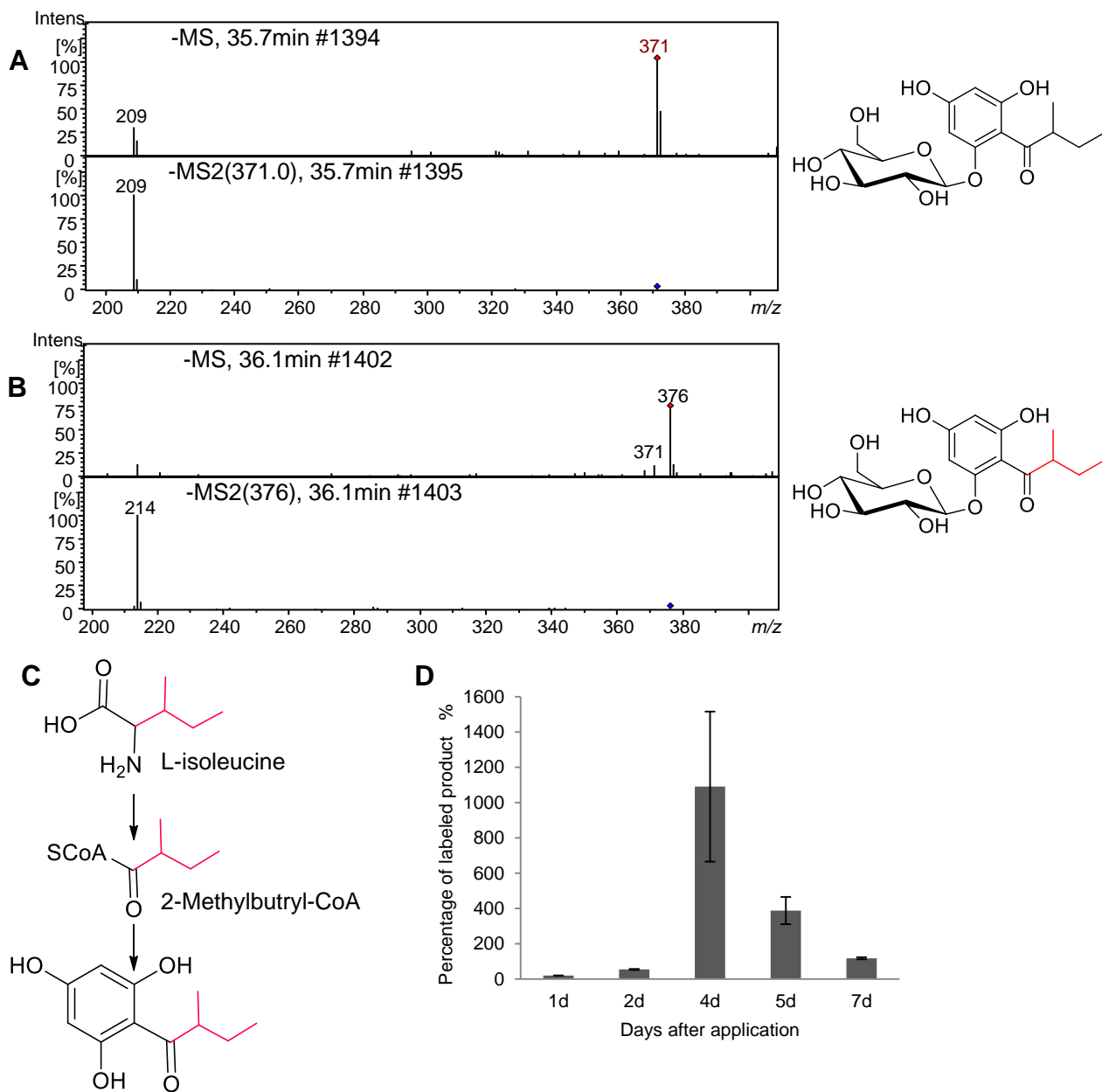


Figure S17. Mass spectrum (MS) and MS2 of unlabeled M1 (**A**) and isotopically labeled M1 (**B**) after application of L-isoleucine-¹³C₆, proposed pathway (**C**), as well as the effect of the incubation period on the accumulation of labeled product (**D**) (percentage of labeled product was calculated from the integrated peak area of the pseudomolecular ion of isotopically labeled product m/z 376; integrated peak area of pseudomolecular ion m/z 371 of unlabeled product was set to 100%).

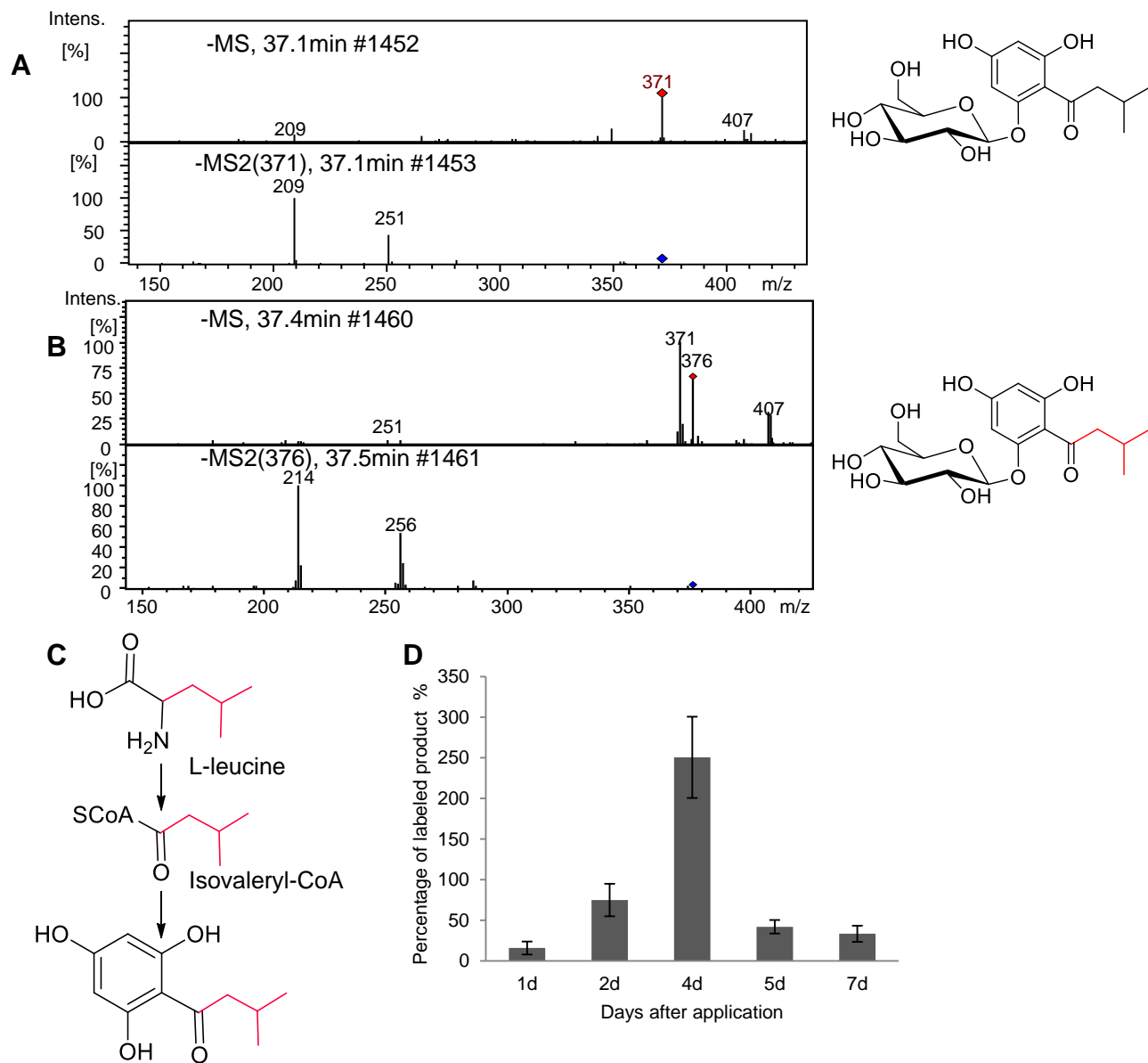


Figure S18. Mass spectrum (MS) and MS2 of unlabeled M3 (**A**) and isotopically labeled M3 (**B**) after application of L-leucine- $^{13}\text{C}_6$, proposed pathway (**C**), as well as the effect of the incubation period on the accumulation of labeled product (**D**) (percentage of labeled product was calculated from the integrated peak area of the pseudomolecular ion of isotopically labeled product m/z 376; integrated peak area of pseudomolecular ion m/z 371 of unlabeled product was set to 100%).

		10	20	30	40	50							
FvCHS2.1	1	--MVTVEEV	RKAQRAEGPATVLAIGTATPPNCIDQSTYPDYFRITNSEH				48						
FvCHS2.2	1	--					48						
VPS	1	MAS	...QI	...I	...V.A	...FN.ADF	...V.K	50					
HlCHS-H1	1	--		...I	...A	...L.E		48					
		60	70	80	90	100							
FvCHS2.1	49	KAE	LEKEKFQRMCDKSMIKKRYMYL	TEEILKENPSMCEYMAPSLDARQDMV			98						
FvCHS2.2	49						98						
VPS	51	MTD	...K	...E	...T	...LH	...H	...Q	...HL	...N	...NT	...L	10
HlCHS-H1	49	.T	...K	...G	...R	...H	...NL	...A	...E				98
		110	120	130	140	150							
FvCHS2.1	99	VVEI	PKLGGKDAAVKAIKEWGQPKSRITHLVFCTTSGVDMPGADYQLTKLL				14						
FvCHS2.2	99		...E	...K			14						
VPS	101	...V	...E	...IN	...K	...I	...G	...SI	...CA			15	
HlCHS-H1	99	...V	...E	...T	...E	...V						14	
		160	170	180	190	200							
FvCHS2.1	149	GLRPSVKRLMMYQQGCFAGGTVLRRLAKDLAENNRGARVLVVCSEITAVTF					19						
FvCHS2.2	149						19						
VPS	151	...V	...L	...L	...Y	...K	...I	...I	...K	...I	...CI	20	
HlCHS-H1	149			...V	...K		19						
		210	220	230	240	250							
FvCHS2.1	199	RGPSDTHLDSL	VGQALFGDGAAAIIVGSDPLPEV-ERPLFELVSAAQ	TIL			24						
FvCHS2.2	199						24						
VPS	201	...EK	...C	...S	...SSV	...A	...DAS	...G	...I			25	
HlCHS-H1	199	...N	...A	...S	...L	...I	...A	...I	...I	...K	...I	24	
		260	270	280	290	300							
FvCHS2.1	248	PDS	GDGAIDGHLREVGLTFHLLKDV	PGLISK	NIEKSLNEAFKPLNITD	WNS	29						
FvCHS2.2	248						29						
VPS	251	.N	...A	...VT	...A	...R	...Q	...I	...T	...IG	...N	...N	30
HlCHS-H1	248					...V	...G	...S				29	
		310	320	330	340	350							
FvCHS2.1	298	LFWIAHPGGPAILDQVEAKLALKPEKLEATR	HILSEYGNMSSACVLF	FILD			34						
FvCHS2.2	298						34						
VPS	301	I	...EI	...E	...K	...MK	...S	...EM	...C	...S	...F	...V	35
HlCHS-H1	298	...T	...S	...G	...R	...V	...G					34	
		360	370	380	390								
FvCHS2.1	348	E	VRRKSAANGHKT	TGEGLEWGVLF	GFGPGLTVETVVLH	SVSA--	389						
FvCHS2.2	348	...R	...K			...A	--	389					
VPS	351	.M	...KQ	...SKE	...KS	...D	...A	...PTNV				394	
HlCHS-H1	348	.M	...C	...ED	...V			...GI	--			389	

Figure S19. Comparison of the deduced amino acid sequences of CHS enzymes from *F. vesca*, FvCHS2-1 and FvCHS2-2, as well as VPS and HlCHS-H1 from hop. The sequences were aligned using the ClustalW program. The highly conserved active site loop of CHS enzymes, G372FGPG and two Phe residues (Phe215 and Phe265), important in determining the substrate specificity of CHS are boxed. 25